

Applications of the Large Mass Expansion

J. Fleischer¹ A.V. Kotikov^{2 3 4} and O. L. Veretin^{5 6}

Fakultät für Physik, Universität Bielefeld, D-33615 Bielefeld, Germany.

The method of the large mass expansion (LME) is investigated for selfenergy and vertex functions in two-loop order. It has the technical advantage that in many cases the expansion coefficients can be expressed analytically. As long as only one non-zero external momentum squared, q^2 , is involved also the Taylor expansion (TE) w.r.t. small q^2 yields high precision results in a domain sufficient for most applications. In the case of only one non-zero mass M and only one external momentum squared, the expansion w.r.t. q^2/M^2 is identical for the TE and the LME. In this case the combined techniques yield analytic expressions for many diagrams, which are quite easy to handle numerically.

¹ E-mail: fleischer@physik.uni-bielefeld.de

² Particle Physics Laboratory, Joint Institute for Nuclear Research, 141980, Dubna (Moscow Region), Russia

³ E-mail:kotikov@thsun1.jinr.dubna.su

⁴ Supported by Volkswagen-Stiftung under I/71 293

⁵ E-mail:veretin@physik.uni-bielefeld.de

⁶ Supported by BMBF under 05 7BI92P(9)

1. Applications of the presented methods in particle physics

Diagrams with one non-zero mass and only one external q^2 have wide applications in QED and QCD for both selfenergies and vertices. For applications in the electroweak part of the full Standard Model (SM), due to the rather large spectrum of masses, in general one has to apply numerical methods. Often, however, approximations like small fermion masses $m_f^2/m_Z^2 \sim 0$, close vector boson masses $(m_Z^2 - m_W^2)/m_Z^2 \sim 0$ and large top mass $m_Z^2/m_t^2 \sim 0$ etc. are considered. In these approximations the problem is often reduced to diagrams with one non-zero mass, which is a further reason for the interest in this type of diagrams. For applications in the electroweak part of the full SM, two calculations in the two-loop order are of particular interest:

a) Z decay into $b\bar{b}$ (bottom, anti-bottom)

The kinematics in this case is $q^2 = M_Z^2$ and $p_1^2 = p_2^2 = 0$ (in the $m_b = 0$ approximation).

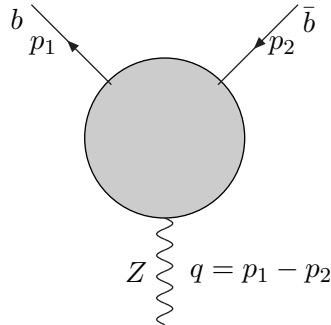


Fig. 1. Kinematics for the decay $Z \rightarrow b\bar{b}$.

We mention that the decay $Z \rightarrow b\bar{b}$ was considered by a number of authors [1] in the limit of large top mass, i.e. in the leading order only the top mass was kept non-zero and all other masses put to zero and even $q^2 = m_Z^2 = 0$. This is an example of the above mentioned approximations and here also the number of diagrams is quite low (of the order of 10). Recently higher order terms in the large top mass expansion have been considered [2] (see also these proceedings). In [3] an investigation of the precision of the higher orders in the large mass expansion has been performed for scalar diagrams occurring in this process and a repetition of higher orders in the large top mass for the full process is under consideration.

b) Anomalous magnetic moment (AMM) of the muon ($g - 2$)

Here the kinematics is quite different, namely $q^2 = 0$ (actually $q = 0$) and $p_1^2 = p_2^2 = m_\mu^2$. In fact in this case the problem reduces to the calculation of two-point functions. In both cases a) and b) we have one external variable only: $q^2 = M_Z^2$ and $p_1^2 = p_2^2 = m_\mu^2$, respectively.

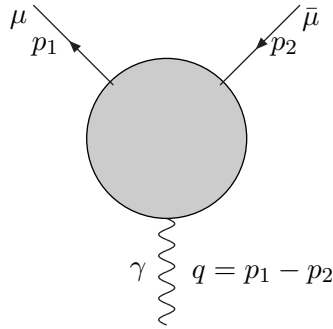


Fig. 2. Kinematics for anomalous moment $(g - 2)_\mu$.

In the case of the AMM our first step was dedicated to an automatic set up of the contributing Feynman diagrams. For this purpose the package TLAMM was developed [4]. Also the large mass expansion (LME) [5] applied to a “toy model” for the $(g - 2)_\mu$ was described in [4], i.e. for diagrams of the selfenergy type. In this model 40 diagrams were contributing to the two-loop AMM of the muon.

In general, however, in the above cases many more, i.e. of the order of 1000 diagrams contribute and naturally it is necessary to investigate diagrams with various non-zero masses.

As was already started with TLAMM, in the full SM it is even more required to produce the Feynman diagrams automatically. Instead of 40 diagrams, e.g., in the above mentioned “toy model” in the full $(g - 2)_\mu$ calculation 1832 diagrams contribute. Such a more general program, called **DIANA** (for DIagram ANALyser) [6], written in C and making use of Nogueira’s QGRAF [7], was also developed in our group. It produces FORM [8] input for the Feynman diagrams according to the Feynman rules for further evaluation.

2. Evaluation of scalar diagrams

In the following we shortly review the main techniques we applied, namely the Taylor expansion (TE) [9] and the LME [5]. The efficiency of both approaches will be compared.

2.1. The Taylor expansion method

Taylor series expansions in terms of one external momentum squared, q^2 say, were considered in [10], Padé approximants were introduced in [11] and in Ref. [9] it was demonstrated that this approach can be used to calculate Feynman diagrams on their cut by analytic continuation. In the case of a three-point function like $Z \rightarrow b\bar{b}$ we have two independent external momenta in $d = 4 - 2\varepsilon$ dimensions. The general expansion of (any loop) scalar 3-point function with its momentum space representation $C(p_1, p_2)$ can be written as

$$C(p_1, p_2) = \sum_{l,m,n=0}^{\infty} a_{lmn} (p_1^2)^l (p_2^2)^m (p_1 p_2)^n \quad (1)$$

where the coefficients a_{lmn} are to be determined from the given diagram. Considering $Z \rightarrow b\bar{b}$ with $m_b = 0$, i.e. $p_1^2 = p_2^2 = 0$, which is a good approximation, only the coefficients a_{00n} are needed. For the calculation of the Taylor coefficients in general various procedures have been proposed [9],[12],[13]. These methods are well suited for programming in terms of a formulae manipulating language like FORM. Such programs, however, yield acceptable analytic results only in cases when not too many parameters (like masses) enter the problem. Otherwise numerical methods are needed [14], [15].

In the case of only one non-zero mass and only one external momentum squared, indeed the case with the least nontrivial parameters, for many diagrams analytic expressions for the Taylor coefficients can be obtained. In Sect. 5 we present some recent results.

For the purpose of calculating Feynman diagrams in the kinematical domain of interest it is necessary to calculate them from the Taylor series on their cut. This is performed by analytic continuation in terms of a mapping.

Assume, the following Taylor expansion of a scalar diagram or a particular amplitude is given $C(p_1, p_2, \dots) = \sum_{m=0}^{\infty} a_m y^m \equiv f(y)$ and the function on the r.h.s. has a cut for $y \geq y_0$.

The method of evaluation of the original series consists in a first step in a conformal mapping of the cut plane into the unit circle and secondly the

reexpansion of the function under consideration into a power series w.r.t. the new conformal variable. A variable often used is

$$\omega = \frac{1 - \sqrt{1 - y/y_0}}{1 + \sqrt{1 - y/y_0}}. \quad (2)$$

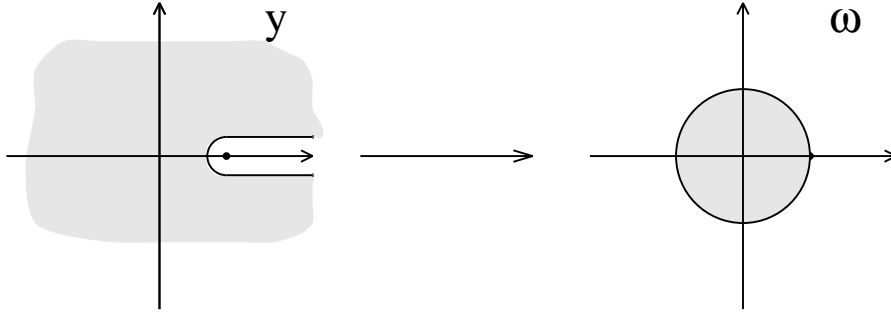


Fig. 3. Conformal mapping of the complex y -plane into the ω -plane.

By this conformal transformation, the y -plane, cut from y_0 to $+\infty$, is mapped into the unit circle (see Fig.3) and the cut itself is mapped on its boundary, the upper semicircle corresponding to the upper side of the cut. The origin goes into the point $\omega = 0$.

After conformal transformation it is suggestive to improve the convergence of the new series w.r.t. ω by applying the Padé method [16],[17]. A convenient technique for the evaluation of Padé approximations is the ε -algorithm of [16] which allows one to evaluate the Padé approximants recursively.

2.2. Large mass expansion (LME)

In particular for the evaluation of diagrams with several different masses, one of which being large (like the top mass, e.g., m_t), we use the general method of asymptotic expansion in large masses [5]. For a given scalar graph G the expansion in large mass is given by the formula

$$F_G(q, M, m, \varepsilon) \stackrel{M \rightarrow \infty}{\sim} \sum_{\gamma} F_{G/\gamma}(q, m, \varepsilon) \circ T_{q^\gamma, m^\gamma} F_\gamma(q^\gamma, M, m^\gamma, \varepsilon), \quad (3)$$

where γ 's are subgraphs involved in the LME, G/γ denotes shrinking of γ to a point; F_γ is the Feynman integral corresponding to γ ; T_{q^γ, m^γ} is

the Taylor operator expanding the integrand in small masses $\{m_\gamma\}$ and external momenta $\{q_\gamma\}$ of the subgraph γ ; \circ stands for the convolution of the subgraph expansion with the integrand $F_{G/\gamma}$. The sum goes over all subgraphs γ which (a) contain all lines with large masses, and (b) are one-particle irreducible w.r.t. light lines.

For the $Z \rightarrow b\bar{b}$ decay we have $q^2 = M_Z^2$ for the on-shell Z 's. Fig.4 shows diagrams with two different masses on virtual lines, one of which is a top. W and Z are the gauge bosons with masses M_W and M_Z , respectively; ϕ is the charged would-be Goldstone boson (we use the Feynman gauge); t and b are the t- and b-quarks.

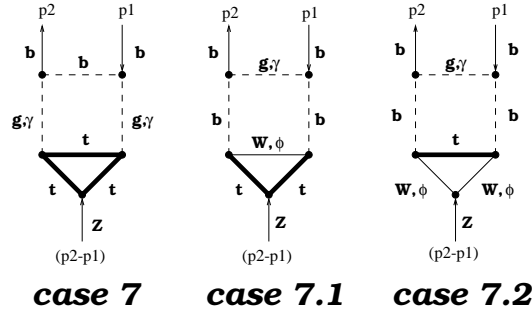


Fig. 4. Two-loop diagrams with two different masses in internal lines arising in the process $Z \rightarrow b\bar{b}$. The notation for the diagrams is chosen according to [9].

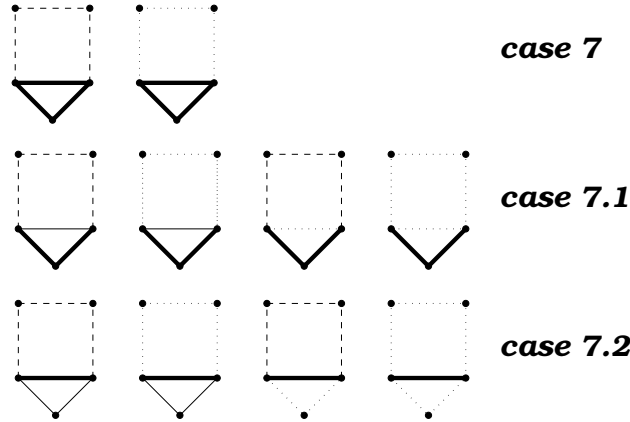


Fig. 5. The structure of the LME, see explanations in the text.

Applying the method of the LME, M_W and M_Z are considered as small. In the framework of this expansion contributions from additional subgraphs

are to be taken into account together with the Taylor expansion of the initial diagrams w.r.t. external momenta and light masses. These are shown in Fig.5. Bold, thin and dashed lines correspond to heavy-mass, light-mass, and massless propagators, respectively. Dotted lines indicate the lines omitted in the original graph Γ to yield the subgraph γ . Γ/γ (see (3)) then consists out of all the dotted lines after shrinking γ to a point.

These subgraphs restore the analytic properties of the initial diagrams (like logarithmic behaviour). In other words, the Taylor expansion of the initial diagrams produces extra infrared singularities which are compensated by singularities of the additional subgraphs so that only the singularities of the original diagrams survive.

At this point it also becomes clear what the difference is between the small- q^2 expansion and what is called here the LME: in the former case we assume all masses large, i.e. $q^2 \ll M_W^2, M_Z^2, m_t^2$ while in the latter case only m_t is considered as large and all other parameters small, i.e. $q^2, M_W^2, M_Z^2 \ll m_t^2$. In this sense both methods are LM expansions. The technical advantage of the second method is, however, that only bubbles with one mass occur, which can be expressed in terms of Γ functions, while in the case of the small q^2 expansion bubbles with different masses are involved, which are much more difficult to evaluate, in fact only numerically. Of course also the number and structure of the subgraphs is different in the two cases.

Finally the LME of the above diagrams has the following general form:

$$F_{\text{as}}^N = \frac{1}{m_t^4} \sum_{n=-1}^N \sum_{\substack{i,j=-1 \\ i+j=n}}^n \left(\frac{M_W^2}{m_t^2} \right)^i \left(\frac{q^2}{m_t^2} \right)^j \sum_{k=0}^m A_{i,j,k}(q^2, M_W^2, \mu^2) \ln^k \frac{m_t^2}{\mu^2} \quad (4)$$

where m is the highest degree of divergence (ultraviolet, infrared, collinear) in the various contributions to the LME ($m \leq 3$ in the cases considered). M_W^2/m_t^2 and q^2/m_t^2 are considered as small parameters. $A_{i,j,k}$ are in general complicated functions of the arguments, i.e. they may contain logarithms and higher polylogarithms.

In the next Section we present results and compare the two methods described here.

3. Results

The small momentum expansion of cases 7, 7.1 and 7.2 is described in detail in Ref. [15]. The additional subgraph arising in these cases is the same irrespectively of the mass distribution and is shown in Fig.5 (*case 7*).

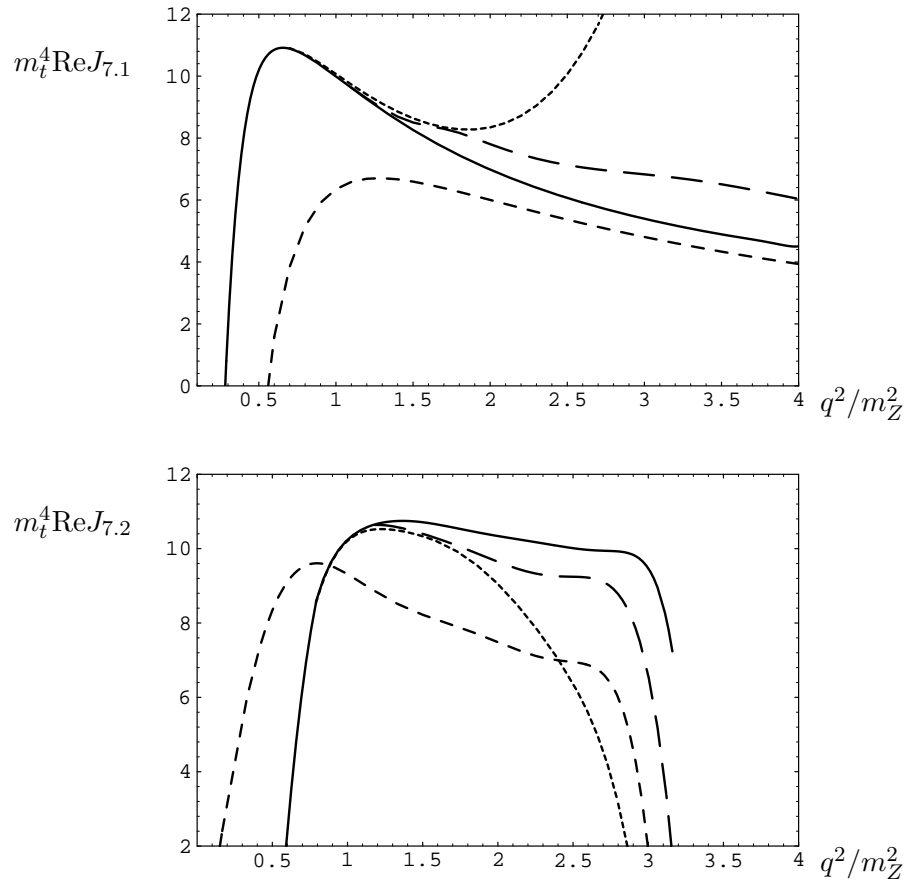


Fig. 6. Results of the LME for the real finite parts of diagrams 7.1 and 7.2 . Solid curves represent the small- q^2 expansions, middle-dashed the leading term of the LME, short-dashed the sum of 11 terms in the LME, long-dashed the [5/5] Padé approximant from the LME.

In the case of the LME two additional subgraphs arise in each of the cases 7.1 and 7.2. Beyond that these sets of additional subgraphs are also of quite different structure. Furthermore the 2nd and 4th graphs in the row (see Fig.5) produce $1/\epsilon^3$ terms which cancel, however. Since there are no UV divergences, these must be mixtures of infrared and collinear ones. They determine the highest degree of divergence in these cases and thus the highest power of the logarithm as discussed in (4).

Our numerical results for cases 7.1 and 7.2 are presented in Fig.6, and for $q^2 = M_Z^2$ in Table 1. In the figures we show the small q^2 -expansion (solid line) in comparison with the lowest order approximation (middle-

dashed) and the sum of terms (small-dashed) with $N=9$, see (4). The scale parameter $\mu = m_t$, i.e. only $k=0$ contributes in (4). We see that up to $q^2 = M_Z^2$ the sum of 11 terms agrees quite well with the small q^2 -expansion, while for higher q^2 the agreement very quickly worsens. For this reason we formally apply also the Padé summation technique. With 11 terms in the series, a [5/5]-approximant (long-dashed) can be constructed. It is seen that indeed this improves the situation considerably up to $q^2 = 4M_Z^2$ though for a better agreement many more terms in the LME would be needed. In the small q^2 -expansion only 9 terms were taken into account, i.e. a [4/4] approximant is calculated. From Table 1 we see that for $q^2 = M_Z^2$ indeed a rather precise result can be obtained with 11 terms from the LME, in particular if Padé's are applied [3].

$F^{(0)}$ in Table 1 corresponds to the lowest order of the diagrams ($N=-1$ or 0, respectively) and $F^{(4)}$ to the order of expansion performed in Ref. [2].

Table 1. Values of diagrams at $q^2 = 90^2$, $\mu = m_t = 180$, $m_W = 80$.

	case 7.1		case 7.2	
$F^{(0)}$	6.4	-i30.0	9.2	-i24.5
$F^{(4)}$	11.1	-i17.93	9.4	-i44.848
$F^{(10)}$	10.1	-i17.95218	10.122	-i44.84523
[5/5]	9.996	-i17.9528	10.189	-i44.842
small- q	9.992668259	-i17.95215366	10.193902102	-i44.845273975

4. Bremsstrahlung

Of particular interest is the calculation of Bremsstrahlung in terms of the LME. Let us consider again the decay $Z \rightarrow b\bar{b}$. The kinematics of the (gluon-) Bremsstrahlung for this process is given by

$$q \rightarrow p_1 - p_2 + p_3, \quad p_1^2 = p_2^2 = p_3^2 = 0.$$

Thus we have 3 invariants

$$p_1 p_2, \quad p_2 p_3, \quad p_3 p_1.$$

We are interested in the integrated bremsstrahlung. The phase space measure in d dimensions can be written as

$$\begin{aligned} \int d\Gamma_3 &= \int \delta^{(d)}(q - p_1 + p_2 - p_3) \prod_{i=1}^3 \frac{d^{d-1} \mathbf{p}_i}{(2\pi)^{d-1} 2p_{i0}} \\ &= \frac{1}{(2\pi)^{3d-3}} \frac{2(2\pi)^{d-2}}{\Gamma(d-2)} \frac{q^2}{32} \left(\frac{q^2}{2}\right)^{d-4} \\ &\quad \int_0^1 dx dy x^{d-3} (1-x)^{d/2-2} y^{d/2-2} (1-y)^{d/2-2} \end{aligned} \quad (5)$$

and the invariants can be expressed in terms of x, y as

$$\begin{aligned} p_1 p_2 &= \frac{q^2}{2} x(1-y), \\ p_2 p_3 &= \frac{q^2}{2} (1-x), \\ p_3 p_1 &= \frac{q^2}{2} xy. \end{aligned}$$

For the 1-loop amplitude we apply the LME w.r.t the top mass m_t^2 . For the diagrams with M_W and m_t mass in virtual lines the desired expansion looks like

$$A = \sum_N \sum_{i+j+k+n=N} \left(\frac{p_1 p_2}{m_t^2}\right)^i \left(\frac{p_2 p_3}{m_t^2}\right)^j \left(\frac{p_3 p_1}{m_t^2}\right)^k \left(\frac{m_W^2}{m_t^2}\right)^n f_{ijkn}, \quad (6)$$

where f_{ijkn} are cubic polynomials of $\log(m_t^2/\mu^2)$ with coefficients being functions of q^2, m_W^2, μ^2 , i.e.

$$f_{ijkn} = a \log^3 \frac{m_t^2}{\mu^2} + b \log^2 \frac{m_t^2}{\mu^2} + c \log \frac{m_t^2}{\mu^2} + d.$$

After expansion the integration over the phase space is trivial (it can be done completely in terms of Γ -functions).

5. Diagrams with only one non-zero mass

So far the method of expansion is considered as semianalytic in the sense that only a limited number of coefficients can be obtained explicitly. In this Section, however, we want to go one step further. We calculate the first few coefficients of the expansion of a diagram with only one non-zero mass by means of the LME [5] method. The method of differential equations [18] then yields an idea, like in [19], what the general analytic form of these coefficients might be, providing some ‘‘basis’’ in terms of which they might be expressed. The Ansatz of equating the explicit coefficients obtained from the LME to a linear combination in terms of the basis elements, yields a system of linear equations, which can be solved to yield the desired representation of the coefficients.

The main problem in this approach is the choice of the basis elements. We start from so-called harmonic sums which are particularly relevant for moments of structure functions in QCD (e.g. [20]). These functions are

directly related to (generalized) polylogarithms [21] and therefore it is not surprising that they appear in the analysis of massive diagrams. However, not every massive diagram even of self-energy type can be expressed in terms of these sums. Apart from harmonic sums we introduce a new type of sums which we call W - and V -sums.

Our starting point is the LME [5] of the diagrams. For the particular diagrams under consideration it was discussed in detail in [9]. Here we just note that the result of a large mass expansion for these diagrams reads ($z = q^2/m^2$)

$$J = \frac{1}{(q^2)^a} \sum_{n \geq 1} z^n \sum_{j=0}^{\omega} \frac{1}{\varepsilon^j} \sum_{k=0}^{\nu} \log^k(-z) A_{n,j,k}, \quad (7)$$

where a is the dimensionality of the diagram, ω and ν independent of n are the highest degree of divergence and the highest power of $\log(-q^2/m^2)$, respectively (in our cases $\omega, \nu \leq 4$). The coefficients $A_{n,j,k}$ are of the form $r_1 + \zeta_2 r_2 + \dots + \zeta_\nu r_\nu$ with r_c being rational numbers and $\zeta_c = \zeta(c)$ is the Riemann ζ -function.

Series (7) always has a nonzero radius of convergence, which is defined by the position of the nearest nonzero threshold in the q^2 -channel. For brevity we shall call m -cuts ($2m$ -cuts, etc.) possible cuts of a diagram in q^2 corresponding to 1 (2, etc.) massive particles in the intermediate state.

We start from diagrams with the simplest threshold structure, i.e. with m -cuts and 0-cuts. It turns out that all of these with only one massive line are expressible in terms of harmonic sums $S_k(n-1) = \sum_{j=1}^{n-1} 1/j^k$ and alternating harmonic sums $K_a(n-1) = \sum_{j=1}^{n-1} (-)^{j+1}/j^a$.

As a first example consider the 2-loop 2-point function of Fig. 7, $J_{(a)}$, which was considered in [22]. Using the standard large mass expansion technique one can get the first few coefficients of the expansion of this diagram in powers of $z = q^2/m^2$

$$\frac{1}{q^2} \sum_{n=1}^{\infty} a_n z^n = \frac{1}{q^2} \left(2\zeta_2 z + \left(\zeta_2 + \frac{1}{2} \right) z^2 + \left(\frac{2}{3}\zeta_2 + \frac{1}{2} \right) z^3 + \dots \right), \quad (8)$$

where $\zeta_2 = \zeta(2)$ is the Riemann ζ -function.

Our first step is to find an expression for the higher order terms of the series (8) as a functions of n i.e. $a_n = a(n)$.

To achieve this let us search for a_n as a linear combination of harmonic sums. The rule is that one has to take into account all possible products of the type $\zeta_a S_{b_1} \dots S_{b_k} / n^c$ with the 'transcendentality level' (TL) $a + b_1 + \dots + b_k + c = 3$. It is obvious that one can exclude ζ_3 from the very beginning

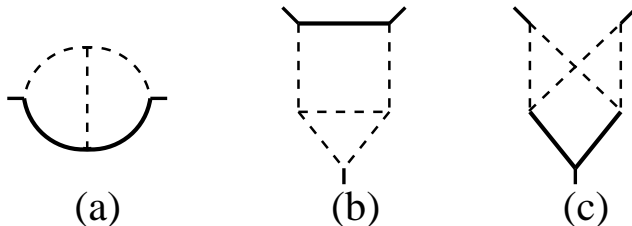


Fig. 7. Three diagrams, selfenergy and vertices, for the TE of which results are reported.

since it never appears on the r.h.s. of (8). Thus we have the following Ansatz for a_n

$$a_n = \frac{\zeta_2}{n}x_1 + \zeta_2 S_1 x_2 + S_3 x_3 + S_2 S_1 x_4 + S_1^3 x_5 + \frac{S_2}{n}x_6 + \frac{S_1^2}{n}x_7 + \frac{S_1}{n^2}x_8 + \frac{1}{n^3}x_9, \quad (9)$$

where x_1, \dots, x_9 are rational numbers independent on n . The argument of the S -functions is $n - 1$. We refer to the structures in (9) as ‘basis elements’. Indeed, the functions $\zeta_a S_{b_1}(n-1) \dots S_{b_k}(n-1)/n^c$ are algebraically independent.

Inserting the expression for a_n from (9) into the l.h.s. of (8) and equating equal powers of z , we obtain a system of linear equations for the x_i . An explicit computation ensures that the system can be solved in terms of rational numbers for the x_i . The solution is $x_1 = 2, x_6 = 2, x_8 = -2, x_{2,3,4,5,7,8} = 0$ i.e. the answer for the diagram at hand is

$$J_{(a)} = \frac{1}{q^2} \sum_{n=1}^{\infty} z^n \left(2 \frac{\zeta_2}{n} + 2 \frac{S_2(n-1)}{n} - 2 \frac{S_1(n-1)}{n^2} \right). \quad (10)$$

Equation (9) can be considered as expansion of the general coefficient a_n in terms of a ‘basis’ with (unknown, rational) coefficients x_i . Now the question arises: what are the basis elements in general? So far we are lacking rules for predicting a basis of a given diagram. The power of the method, however, is that given a set of basis elements for one diagram, it can be used to find the solution for other diagrams. Often, though, one has to ‘generalize’ already known (harmonic) sums in a basis.

As an illustration consider the diagram shown in Fig. 7, $J_{(b)}$. Its large mass expansion looks like

$$J_{(b)} = \frac{1}{(q^2)^2} \sum_{n=1}^{\infty} z^n \left(r_n^{(2)} \log^2(-z) + r_n^{(1)} \log(-z) + r_n^{(0,3)} \zeta_3 + r_n^{(0,2)} \zeta_2 + r_n^{(0,0)} \right), \quad (11)$$

with the r 's being rational numbers. It is obvious that one can search for a solution for each of the r 's independently. Again we use the same set of functions ($1/n^a$ and S_b) as above but now with different transcendentality level(s). The system of equations has a solution only if we add the factor $(-)^n$ which can be seen easily by inspection of the series. At the end we arrive at

$$J_{(b)} = \frac{1}{(q^2)^2} \sum_{n=1}^{\infty} z^n (-)^n \left(\frac{S_1}{n} \log^2(-z) + \left(-4 \frac{S_2}{n} + \frac{S_1^2}{n} - 2 \frac{S_1}{n^2} \right) \log(-z) - 6 \frac{\zeta_3}{n} + 2 \frac{\zeta_2 S_1}{n} + 6 \frac{S_3}{n} - 2 \frac{S_2 S_1}{n} + 4 \frac{S_2}{n^2} - \frac{S_1^2}{n^2} + 2 \frac{S_1}{n^3} \right), \quad (12)$$

where as above we take all harmonic sums (S_i) with the argument $n-1$, which is omitted.

We point out that in (12) the part without $\log(-z)$ has basis elements $\zeta_a S_b / n^c$ obeying $a+b+c=4$ (i.e. it has a basis with TL=4). Terms proportional to $\log(-z)$ are of 3rd level while those proportional to $\log^2(-z)$ are of the 2nd. One can say that $\log(-z)$ itself is of 1st level and each $\log^a(-z)$ reduces the level of basis elements by a units. This is the general behaviour for all diagrams we consider. The same rule applies to UV and IR poles $1/\varepsilon$ if they are present in a diagram i.e. each $1/\varepsilon^a$ reduces the level of basis elements by a units.

We also stress the presence of the factor $(-)^n$. Strictly speaking the basis now is not $\zeta_a S_b / n^c$ but rather $(-)^n \zeta_a S_b / n^c$.

Finally we observe the following recipe of generalization, i.e. elements of higher TL ($a+b$) can be constructed in the form:

$$S_{a,b}(n) = \sum_{j=1}^n \frac{1}{j^a} S_b(j-1), \quad (13)$$

$$K_{a,b}(n) = - \sum_{j=1}^n \frac{(-)^j}{j^a} S_b(j-1). \quad (14)$$

$$(15)$$

The structure of the lowest level for diagrams having both m - and $2m$ -cuts is more complicated. We find it from the nonplanar graph shown in Fig. 7, $J_{(c)}$. Namely this diagram has a double collinear pole and we can easily perform the integrations in calculating the $1/\varepsilon^2$ contribution with the result

$$J_{(c)} \stackrel{1/\varepsilon^2}{=} - \frac{1}{\varepsilon^2 (q^2)^2} \int_0^1 \frac{d\alpha_1 d\alpha_2}{(1-\alpha_1(1-\alpha_2)z)(1-(1-\alpha_1)\alpha_2 z)}$$

$$\begin{aligned}
&= -\frac{1}{\varepsilon^2(q^2)^2} \sum_{n=1}^{\infty} z^n \frac{(n!)^2}{(2n-1)!} 3 \sum_{j=1}^{n-1} \frac{(2j)!}{(j!)^2} \frac{1}{j} \\
&= -\frac{1}{\varepsilon^2(q^2)^2} \sum_{n=1}^{\infty} z^n \binom{2n}{n}^{-1} 6 \frac{W_1(n-1)}{n}. \tag{16}
\end{aligned}$$

If we assign to the factor $\binom{2n}{n}^{-1}$ the 0th level, then the expression on the r.h.s of (16) has the correct 2nd level as it should be for the double pole part of a vertex function. The generalization is done according to

$$W_{a,b}(n) = \sum_{j=1}^n \binom{2j}{j} \frac{1}{j^a} S_b(j-1). \tag{17}$$

$$\tag{18}$$

The result for the diagram under consideration finally is

$$\begin{aligned}
J_{(c)} &= \frac{1}{(q^2)^2} \sum_{n=1}^{\infty} z^n \binom{2n}{n}^{-1} \frac{1}{n} \\
&\left\{ -\frac{6}{\varepsilon^2} W_1 + \frac{1}{\varepsilon} [-4W_2 - 12W_{1,1} - 12S_1W_1 - 16S_2] \right. \\
&\quad -18\zeta_2 W_1 - 4W_3 - 8S_3 + 12W_{1,2} - 8W_{2,1} - 12W_{1,(1+1)} \\
&\quad \left. -16S_{1,2} - 8S_1W_2 - 24S_1W_{1,1} - 16S_1S_2 - 12S_1^2W_1 \right\}, \tag{19}
\end{aligned}$$

where

$$S_{a,(b+c)}(n) = \sum_{j=1}^n \frac{1}{j^a} S_b(j-1) S_c(j-1), \tag{20}$$

$$W_{a,(b+c)}(n) = \sum_{j=1}^n \binom{2j}{j} \frac{1}{j^a} S_b(j-1) S_c(j-1) \text{ etc.}, \tag{21}$$

all have TL= $a + b + c$.

For completeness we mention a further type of basis elements which we discovered from the application of the differential equation method [19]

$$V_a(n-1) = \sum_{j=1}^{n-1} \binom{2j}{j}^{-1} \frac{1}{j^a}. \tag{22}$$

Further basis elements were obtained in a similar fashion. The result for a great variety of diagrams will be published elsewhere.

6. Conclusion

The purpose of many of our investigations is to test various methods for the calculation of two-loop diagrams needed for the evaluation of measured processes in the full SM of the electroweak theory. Comparing different methods yields information about their precision and possible applicability. In particular we have forced the development of packages for the large mass expansion and found that in the domain of interest for the processes under consideration this method can be used with reasonable liability. For the case of only one non-zero mass a completely new approach was found, namely “guess and verify”, to set up analytic expressions for many diagrams of interest.

REFERENCES

- [1] J. Fleischer, O.V. Tarasov, F. Jegerlehner and P. Rączka, Phys. Lett. B293 (1992) 437; G. Buchalla and A.J. Buras, Nucl. Phys. B398 (1993) 285; G. Degrassi, Nucl. Phys. B407 (1993) 271; K.G. Chetyrkin, A. Kwiatkowski and M. Steinhauser, Mod. Phys. Lett. A8 (1993) 2785.
- [2] R.Harlander, T.Seidensticker and M.Steinhauser, hep-ph/9712228, preprint MPI/PhT/97-81, TTP97-52;
- [3] J. Fleischer, M. Kalmykov and O. Veretin, Phys. Lett. B427 (1998) 141.
- [4] L.V. Avdeev, J. Fleischer, M. Yu. Kalmykov, M. Tentyukov, Nucl.Instrum. Meth. A 389 (1997) 343; *Towards Automatic analytic Evaluation of Diagrams with Masses*, Comp.Phys.Comm. 107 (1997) 155.
- [5] F.V. Tkachov, Preprint INR P-0332, Moscow (1983); P-0358, Moscow (1984); K.G. Chetyrkin, Teor. Math. Phys. 75 (1988), 26; ibid 76 (1988), 207; Preprint, MPI-PAE/PTh-13/91, Munich (1991); V.A. Smirnov, Comm. Math. Phys. 134 (1990), 109; *Renormalization and asymptotic expansions* (Birkhäuser, Basel, 1991).
- [6] L.V. Avdeev, J. Fleischer, M. Yu. Kalmykov, M. Tentyukov, Nucl.Instrum. Meth. A 389 (1997) 343; *Towards Automatic analytic Evaluation of Diagrams with Masses*, accepted for publication in Comp.Phys.Comm.,(hep-ph/9710222); L.V. Avdeev, M.Yu. Kalmykov, Nucl. Phys. B502 (1997) 419; J. Fleischer and M. Tentukov, *A Feynman Diagram Analyser DIANA*, in preparation.
- [7] P. Nogueira, J. Comput. Phys. 105 (1993), 279.

- [8] J.A.M. Vermaseren: Symbolic manipulation with FORM, Amsterdam, Computer Algebra Nederland, 1991.
- [9] J. Fleischer and O.V. Tarasov, *Z.Phys.*, **C 64** (1994) 413; J.Fleischer and O.V.Tarasov, in proceedings of the ZiF conference on *Computer Algebra in Science and Engineering*, Bielefeld, 28-31 August 1994, World Scientific 1995, J. Fleischer, J. Grabmeier, F.W.Hehl and W.Küchlin editors. J. Fleischer, V. A. Smirnov and O. V. Tarasov, *Z.Phys.***C74** (1997) 379.
- [10] A.I. Davydychev and J.B. Tausk, *Nucl. Phys.*, **B397** (1993) 123.
- [11] D.J. Broadhurst, J. Fleischer and O.V. Tarasov, *Z.Phys.*, **C 60** (1993) 287.
- [12] A.I. Davydychev and J.B. Tausk, *Nucl. Phys.*, **B465** (1996) 507.
- [13] O.V. Tarasov, *Nucl. Phys.*, **B480** (1996) 397.
- [14] J. Fleischer, *Int.J.Mod.Phys.***C6** (1995) 495;
- [15] J. Fleischer et al., *Eur.Phys.J. C2* (1998) 747.
- [16] D. Shanks, *J. Math. Phys.* **34** (1955); P. Wynn, *Math. Comp.* **15** (1961) 151; G.A. Baker, P. Graves-Morris, Padé approximants, in *Encycl.of math.and its appl.*, Vol. **13, 14**, pp Addison-Wesley (1981).
- [17] G.A. Baker, Jr., J.L. Gammel and J.G. Wills, *J.Math.Anal.Appl.*, **2** (1961) 405; G.A. Baker, Jr., *Essentials of Padé Approximants*, pp Academic Press (1975).
- [18] A.V. Kotikov, *Phys.Lett.* **B254** (1991) 185; *ibid.* **B259** (1991) 314; *ibid.* **B267** (1991) 123.
- [19] J. Fleischer, A.V. Kotikov and O.L. Veretin, *Phys.Lett.* **B417** (1998) 163.
- [20] A. González-Arroyo, C. López and F.J. Ynduráin, *Nucl. Phys.* B153 (1979) 161; J.A.M. Vermaseren, NIKHEF-98-14, hep-ph/9806280.
- [21] A.Devoto and D.W.Duke, *La Rivista del Nuovo Cimento*, Vol. 7, No. 6 (1984) 1; K.S. Kölbig, *SIAM Journal on Mathematical Analysis*, Vol. 17, No. 5 (1986) 1232.
- [22] D.J. Broadhurst, *Z.Phys.* **C47** (1990) 115.